Anomalously low thermal conductivity in superhard cubic-Si_3N_4

Jing Liu[1], Shenghong Ju[1,2], Norimasa Nishiyama[3], Shiomi Junichiro[1,2,*]

[1]Department of Mechanical Engineering, The University of Tokyo, 7-3-1 Hongo, Bunkyo, Tokyo 113-8656, Japan

[2]Center for Materials research by Information Integration (CMI2), Research and Services Division of Materials Data and Integrated System (MaDIS), National Institute for Materials Science (NIMS), 1-1 Namiki, Tsukuba, Ibaraki 305-0044, Japan

[3]Laboratory for Materials and Structures, Tokyo Institute of Technology, 4259 Nagatsuta-cho, Midori-ku, Yokohama 226-8503, Japan.

ABSTRACT

Super hard bulk materials with large bulk modulus like diamond and cubic BN (c-BN) show high thermal conductivity (κ) reaching 2000-3000 $Wm^{-1}K^{-1}$. The large modulus means large group velocity, which contributes to high lattice thermal conductivity. However, whether the hardening of phonon bands would increase or decrease the phonon scattering rate through the phonon-phonon scattering phase space is not evident and should depend on the material kind. In this work, we target cubic silicon nitride (c-Si_3N_4), which was recently developed and found to be the third super hardest materials next to the diamond and c-BN. The κ of polycrystalline c-Si_3N_4 was measured by time domain thermoreflectance method, and thermal conductivity of 23 $Wm^{-1}K^{-1}$ was obtained at room temperature. The first-principles

* Corresponding email: shiomi@photon.t.u-tokyo.ac.jp

thermal conductivity calculations identified that this translates to single-crystal value of about 88 $Wm^{-1}K^{-1}$, which is more than an order of magnitude smaller than those of diamond and c-BN. The calculation further identified that difference arises from that the large scattering phase space and anharmonic amplitude of c-Si_3N_4 which are 2-3 times larger than the values of diamond. It is found that the scattering phase space of c-Si_3N_4 optical phonons with small dispersion anomalously increases with the frequency.

I. INTRODUCTION

There is a common understanding that the thermal conductivity (κ) positively correlates with the hardness. The large modulus means large group velocity, which contributes to high lattice thermal conductivity. Representative examples are diamond and cubic boron nitride (c-BN) that are the top two hardest materials [1-3] and exhibit extremely high thermal conductivity [4]. The thermal conductivity of single crystalline diamond calculated from first-principles is as high as 3450 $Wm^{-1}K^{-1}$ at room temperature [4], while the κ of isotopically pure diamond obtained by experiment can reach 2270 $Wm^{-1}K^{-1}$ at room temperature [5,6]. c-BN has a high κ of ~ 2000 $Wm^{-1}K^{-1}$ from first-principles study and κ of 768 $Wm^{-1}K^{-1}$ from experiment [4,7,8].

Apart from the hardness, there are other factors that possibly plays role in determining the thermal conductivity according to Slack's criteria: (1) low atomic mass, (2) strong interatomic bonding, (3) simple crystal structure and (4) low anharmonicity [8]. Criteria (1) and (3) usually imply high Debye temperature [6], which corresponds to high cut-off

frequency of phonons. Criterion (3) indicates fewer phonon bands compared with complex crystal structure, which leads to smaller phonon scattering rates. Criteria (4) was put forward due to the fact that the thermal resistance in nonmetallic crystal arises from the anharmonic phonon-phonon scattering at room temperature. Therefore, some superhard materials may have counterintuitively limited thermal conductivity when other factors become dominant.

It is important to note here that Slack's criteria do not provide quantitative measures of which criterion have how much absolute or relative impact to thermal conductivity. Recently, the Slack's criteria were challenged by reported high thermal conductivity materials of boron arsenide (BAs). The thermal conductivity of BAs was theoretically predicted to be 2240 $Wm^{-1}K^{-1}$ [4] and 1400 $Wm^{-1}K^{-1}$ after including four-phonon scattering [9], and then experimentally confirmed to exceed 1000 $Wm^{-1}K^{-1}$ at room temperature despite that it has relatively large average atomic mass and intermediate atomic bonding [10-12]. The high thermal conductivity was attributed to the band gap between acoustic and optical phonons [4], which suggests that one of the Slack's criteria can overwhelm the others. Therefore, quantitative case studies of specific superhard materials are need to gain understanding in thermal conductivity and underlying mechanism.

In this work, we particularly targeted superhard crystals with strong interatomic bonds. The lattices of super hard materials are more resistant to deformation due to the strong interatomic bonds [13,14], which leads to low anharmonicity in materials [13,14]. Silicon nitride (Si_3N_4) is a newly developed super hard material, which has three polymorphs: α, β and γ phases. α-Si_3N_4 or β-Si_3N_4 are the thermo-dynamically stable phases with hexagonal

structures at ambient condition. The γ phase Si_3N_4 which is also called cubic-Si_3N_4 (c-Si_3N_4) shows a cubic spinel structure [15]. c-Si_3N_4 is recognized as the third hardest material next to diamond and c-BN [1,2], with the potential application including cutting tools, anti-friction bearings [15], and optic windows under extreme condition [2]. The bond strengths of C-C, B-N and Si-N were reported to be 610 [16], 389 [16], and 470 kJ/mol [17], and thus, the strength of interatomic bond of c-Si_3N_4 is in between those of diamond (C-C) and c-BN (B-N). Even though c-Si_3N_4 has large bulk modulus, the previous first-principles thermal conductivity calculation of c-Si_3N_4 has shown that κ is not as high as those of diamond and c-BN, suggesting that bulk modulus may not be a good indicator of thermal conductivity [18].

Here, we report the κ of polycrystalline c-Si_3N_4 measured by time-domain thermoreflectance (TDTR) method. First-principles single-crystal calculation is further performed to investigate the underlying mechanism governing the κ of c-Si_3N_4, by comparing the phonon group velocity, the phonon relaxation time, phonon scattering phase space, and anharmonic amplitude with those of diamond and c-BN. The consistency between the experiment and calculation is finally confirmed by extending the calculation to polycrystalline c-Si_3N_4 using an empirical model.

II. EXPERIMENT

A. Sample fabrication and structure analysis

The starting material for fabrication of the polycrystalline c-Si_3N_4 is commercially available α-Si_3N_4 powder (SN-E10., Ube Industries, Ltd., Ube, Japan), which is not isotope-enriched. The as-received powder was first dried for 8 hours under 200 °C and then enclosed

into a sample capsule. After loading the capsule into a MgO sleeve with MgO lids, the assembled sample container was dried in the vacuum oven for 2 hours under 150 °C. A Kawai-type apparatus, installed at DESY, with a Walker-module (mavo press LPR 1000-400/50; Max Voggenreiter GmbhH, Mainleus, Germany) was used to offer the high pressure (15.6 GPa) and high temperature ambient (1700-1800 °C) for the sample synthesis. More details of the fabrication process are described in the previous report [2]. The unit cell parameter of c-Si_3N_4 was determined by the XRD pattern: a= 7.7373 ± 0.0006Å, which is consistent with former research [19]. Both the unit cell parameter and density of our sample indicate that the sample is in cubic phase [2]. From the TEM image, the sample was found to be polycrystalline with the average grain size of 143 ± 59 nm [2]. More details about structure analysis can be found also in the previous report [2].

B. Thermal conductivity measurement

Two-color TDTR method was employed to measure the κ of polycrystalline c-Si_3N_4. TDTR is a well-developed method, which utilizes the pulsed pump beam centered at 400 nm and probe beam centered at 800 nm to characterize the thermal transport [20-22]. First, the smoothed side of the c-Si_3N_4 sample was coated with an Al transducer film by vacuum evaporation. During the measurement, a pulse train of pump beam was first irradiated to the sample from the Al-transducer side. The temperature evolution of the transducer was sensed by the probe beam with certain delay time. A lock-in amplifier was used to detect the intensity of the reflected probe beam, which was proportional to the temperature. The detected signal includes two parts: in phase signal (V_{in}) and out of phase signal (V_{out}). The ratio $R = -V_{in}/V_{out}$ was fitted to the solution of the physical model (heat conduction equation) to extract the

unknown parameters. The thickness of Al, heat capacity (ρC_p) and κ of Al film that were either known or measured in advanced were input to the physical model. Then the remaining two unknown parameters, κ and interface thermal conductance between Al and c-Si_3N_4, were extracted by the fitting. The fitting curve is shown in Fig. 1(a). The robustness of the fitting was checked by analyzing the sensitivity $S_{R,x} = \frac{d\ln R}{d\ln x}$, where x is the target parameter. As shown in Fig. 1(b), R is sensitive to the changes of sample thermal conductivity and interface thermal conductance between polycrystalline c-Si_3N_4 and Al film, and thus, it is valid and trustworthy to fit the two parameters simultaneously. As the result, the κ of polycrystalline c-Si_3N_4 and the interface thermal conductance between Al and polycrystalline c-Si_3N_4 were obtained to be 23.0 ± 1.6 $Wm^{-1}K^{-1}$ and 62.0 ± 4.5 $MWm^{-2}K^{-1}$, respectively. The κ of polycrystalline c-Si_3N_4 is two order of magnitude smaller than the thermal conductivity of superhard materials like diamond and c-BN.

III. THEORETICAL ANALYSIS

A. Lattice thermal conductivity calculations

We performed bulk thermal conductivity calculation of c-Si_3N_4 based on anharmonic lattice dynamics using IFCs obtained from first principles [23-25]. To obtain both the harmonic and anharmonic IFCs using the real-space displacement method, we adopted 2 × 2 × 2 conventional supercell containing 448 atoms. The density-functional theory (DFT) calculations were performed using Quantum ESPRESSO with revised Perdew-Burke-Ernzerhof exchange-correlation functions based on generalized gradient approximation (GGA) that improves equilibrium properties for solids (PBEsol) [26,27]. The kinetic energy

cutoff was 60 and 400 Ry, respectively, for wave functions and charge density with the ***k***-mesh of 2 × 2 × 2. Using the IFCs, phonon relaxation time were calculated by the anharmonic lattice dynamics (ALD) method rigorously solving the Fermi's Golden rule for phonon self-energies. The Boltzmann transport equation (BTE) with relaxation time approximation (RTA) was employed to calculate the κ. The ALD and BTE calculations were performed using the ALAMODE package [28]. The theoretical κ of single crystalline c-Si_3N_4, diamond, and c-BN as a function of temperature are plotted in Fig. 2. After accounting for the isotope scattering due to the nature isotope distribution using Tamura's model [29], the calculated thermal conductivity of c-Si_3N_4 at room temperature is 88 $Wm^{-1}K^{-1}$. This result is consistent with 81 $Wm^{-1}K^{-1}$ of Tatsumi et al. obtained by similar ALD-BTE calculations using first-principles IFCs including the same isotope scattering [14]. The values are different from 272 $Wm^{-1}K^{-1}$ recently reported by Xiang et al. [30]. But that could be due to the approximation in the modified Debye-Callaway's model used in their work [31]. Recently, four-phonon scattering has been reported to play an important role in reducing the thermal conductivity of crystals [9,32]. Previous works have found that the four-phonon scattering process becomes important under high temperature and materials with high thermal conductivity or acoustic-optical phonon band gaps [9,33]. In this work, since we mainly focus on the thermal conductivity of c-Si_3N_4 at RT and c-Si_3N_4 does not exhibit the band gap, only three-phonon scattering process was considered. In Table 1, the mechanical properties and κ of c-Si_3N_4 at 300 K are compared with those of diamond and c-BN. Despite that c-Si_3N_4 is ranked as the third hardest material, its κ is only about 2.6% of that of diamond, and 4.2% of that of c-BN at room temperature [4].

B. Scattering phase space and anharmonic amplitude

It is well known that in nonmetallic materials, the thermal resistance at high temperature rises by the phonon-phonon scattering. Figure 3(a) shows the phonon dispersion relation of c-Si_3N_4. In a primitive cell, c-Si_3N_4 has 42 phonon modes while diamond and c-BN only have 6 phonon modes. More optical phonon bands in the c-Si_3N_4 is expected in general to offer more phonon scattering channels when compared with those of diamond and c-BN. For quantitative analysis, phonon group velocities of the c-Si_3N_4, diamond and c-BN in frequency domain are illustrated in Fig. 3(b). Here, the average group velocities are obtained from the acoustic phonons since they mainly contribute to thermal conductivity. The average phonon velocity in c-Si_3N_4 is 5001 m/s, while those in diamond and c-BN are 9241 m/s and 8240 m/s, respectively. Thus, the squared average group velocity of c-Si_3N_4 is 30 % of that of diamond. The difference in phonon velocities partly contribute to the lower thermal conductivity in c-Si_3N_4 when compared with diamond. However, phonon velocity is not the decisive reason leading to low κ in c-Si_3N_4 considering the fact that the κ of c-Si_3N_4 is 3 % of that of diamond. We thus hypothesize that there is a significant influence from the relaxation time difference.

To clarify the above hypothesis, the relaxation time of single crystal c-Si_3N_4 was calculated for the three-phonon scattering process as shown in Fig. 3(c). As frequency increases, the relaxation time decreases from 100 ps to 1 ps for single crystal c-Si_3N_4. As a comparison, the phonon lifetime in diamond decreases from 1000 ps to 10 ps as frequency increases from 1 THz to 30 THz [34]. It is easily concluded that the extremely short phonon relaxation time is the main cause for the low κ in c-Si_3N_4. To further explore the fundamental

reason for the difference in the phonon relaxation time, we need to revisit what impacts the relaxation time. The relaxation time for each phonon mode is determined by the Bose-Einstein distribution, scattering phase space ($P_3(\omega)$) and anharmonic amplitude ($V_3(\omega)$) [35]. Here, ω is the phonon frequency. The scattering phase space describes the amount of the phonon scattering channels [36]. More phonon scattering channels lead to larger P_3 and shorter phonon relaxation time. Anharmonic amplitude indicates the strength of anharmonicity of each three-phonon scattering process. The anharmonic amplitude in frequency domain can be estimated by $1/(\tau(\omega)P_3(\omega))$ [36]. The details of the calculation of anharmonic amplitude can be found in the Appendix. Here τ is the phonon relaxation time. In the following, we explore the impact of the scattering phase space (SPS) and anharmonic amplitude on determining the relaxation time.

Three-phonon scattering process, which was constrained by the momentum and energy conservation was considered when calculating the SPS [37]. Figure 4(a) shows the P_3 in frequency domain for c-Si_3N_4, diamond, and c-BN. It is seen that although the P_3 of c-Si_3N_4 is similar to those of diamond and c-BN in the low frequency regime, at the frequency exceeds about 15 THz, P_3 of c-Si_3N_4 anomalously increases and becomes considerably larger than those of diamond and c-BN. We expect this to be due to the flat phonon bands in phonon dispersion relations (Fig. 3(a)) arising from the complex unit cell of c-Si_3N_4 (39 optical phonon branches). Figure 2(b) shows the dependence of cumulative κ on frequency for c-Si_3N_4. The phonons with frequency higher than 20 THz hardly contribute to the thermal conductivity. Instead, these phonons act as the scatters for lower frequency phonons to suppress the thermal conductivity. To confirm that such scattering processes are important in

determining the thermal conductivity of c-Si_3N_4, we have performed calculations by artificially turning off the specific group of three-phonon scattering processes [36], AAA, AAO, AOO, and OOO, where "A" and "O" denote acoustic and optical phonons. As shown in Fig. 5, it is found that the dominating process that limits the thermal conductivity in deed is AOO, where at least one of the optical phonons is expected to have high frequency. c-Si_3N_4The anharmonic amplitude in frequency domain is shown in Fig. 4(b). The detailed description of anharmonic amplitude calculation can be found in the supplementary materials [38]. For c-Si_3N_4, V_3 increases with increasing frequency in the entire frequency domain, whereas in the case of diamond and c-BN, V_3 increases only minutely until the frequency reaches about 20 THz, and then it begins to increase with a gradient similar to c-Si_3N_4. The total P_3 and average V_3 for c-Si_3N_4, diamond and c-BN are summarized in Table 1. We can find that both the total P_3 and average V_3 of c-Si_3N_4 are 260 % and 190 % of diamond, respectively. Together with the above result that the average group velocity of c-Si_3N_4 is 30 % of diamond, estimating the thermal conductivity as $\kappa \sim v^2/(P_3V_3)$, the ration of thermal conductivity becomes 6 %, which reasonably agrees with the actual value 3%. Therefore, it is concluded that the phonon scattering space and anharmonic amplitude play equal roles in suppressing the thermal conductivity of c-Si_3N_4 with respect to diamond.

C. Theoretical thermal conductivity of polycrystalline c-Si_3N_4

In order to check the consistency between the experiment and calculation, we have extended the thermal conductivity calculation to incorporate also phonon impurity scattering by imperfection of the actual sample and boundary scattering at the polycrystalline grain

boundaries. According to the phonon kinetic gas theory, the thermal conductivity (κ_{poly}) can be expressed as:

$$\kappa_{\text{poly}} = \frac{1}{3V}\sum_{\mathbf{k},s} C_{\mathbf{k},s} v_{\mathbf{k},s}^2 \tau_{\mathbf{k},s}. \quad (1)$$

Here, V is the volume of primitive cell. C, v and τ are heat capacity, phonon velocity and phonon relaxation time, respectively. $\mathbf{k}$ and s are phonon wave vector and phonon polarization, respectively. By adopting to the Mattheissen's rule, the effective relaxation time of a polycrystalline can be written as:

$$\tau(\mathbf{k}, s)^{-1} = \tau_{\text{ph-ph}}(\mathbf{k}, s)^{-1} + \tau_{\text{imp}}(\mathbf{k}, s)^{-1} + \tau_{\text{B}}(\mathbf{k}, s)^{-1}, \quad (2)$$

Here, $\tau_{\text{ph-ph}}$, τ_{imp} and τ_{B} are the relaxation time due to phonon-phonon scattering, phonon-impurity (including vacancy and oxygen contaminates) scattering and phonon-boundary scattering, respectively. Here, the phonon-impurity scattering were calculated using the Tamura model [29]. While the chemical composition of the sample measured by energy dispersive spectroscopy was Si: 60.1 ± 0.3 wt%; N: 37.1 ± 0.4 wt%; O: 2.5 ± 0.2 wt%, assuming that the lattice structure does not change, and nitrogen is substituted either by oxygen or atom with zero mass (vacancy), judging from the stoichiometry of c-Si_3N_4, we obtain effective composition of $Si_3N_{3.71}O_{0.22}X_{0.07}$, with X indicating vacancy. When adopting the Tamura model, which was derived for isotope impurity and only accounts for mass difference, we ignore the modulation of force field due to the substitution [39]. As for the boundary scattering, we model with the Casimir-limit, where phonon-boundary scattering rate is given as: $\tau_{\text{B}}^{-1} = v/D$. Here v and D are the phonon velocity and the average gain size, respectively. The calculated $\tau_{\text{ph-ph}}$, $\tau_{\text{ph-ph+imp}}$, $\tau_{\text{ph-ph+imp+B}}$ are shown in Fig. 3(d). The impurities

and vacancies suppress the thermal conductivity by shortening the relaxation time of high-frequency phonons. On the contrary, the grain boundaries mostly shorten the relaxation time of low-frequency phonons. The temperature dependence of theoretical κ considering all the phonon scattering processes is also shown in Fig. 2. At room temperature, the theoretical κ is determined to be 31.0 $Wm^{-1}K^{-1}$, boundary which, considering the general boundary scattering model that ignores the detail features of the interface, is reasonably close to 23.0 $Wm^{-1}K^{-1}$ obtained by the experiment.

IV.CONCLUSION

In summary, the thermal conductivity of the third superhard c-Si_3N_4 was measured for the first time by the time-domain thermoreflectance method. The value is 23.0 $Wm^{-1}K^{-1}$ which is almost two orders of magnitude lower than that of super hardest diamond and c-BN. The first-principles anharmonic lattice dynamics calculation reveals that even for single crystal phase the thermal conductivity is 88 $Wm^{-1}K^{-1}$. By further analysis of phonon transport, the low thermal conductivity is attributed to large SPS and anharmonic amplitude in c-Si_3N_4 that are 200-300% of diamond, in addition to the fact that squared average group velocity of acoustic phonons is 30% of that of diamond. For polycrystalline c-Si_3N_4, the thermal conductivity obtained from the theoretical calculation is consistent with the value obtained by experiment. The theoretical analysis also indicates that the impurities and vacancies mostly shorten the phonon relaxation time of high-frequency phonons while the grain boundaries shorten the phonon relaxation time of low-frequency phonons.

ACKNOWLEGDEMENTS

This paper was partially supported by CREST Grant No. JPMJCR16Q5 and the Information Integration Initiative (MI2I) project from the Japan Science and Technology Agency (JST), and KAKENHI Grant No. 16H04274 and Grants No. 19K14902 from the Japan Society for the Promotion of Science (JSPS). The calculations in this paper were performed using supercomputer facilities of the Institute for Solid State Physics, the University of Tokyo.

TABLE I. Summary of mechanical properties and thermal properties of super hard materials. B: bulk modulus, G: shear modulus, H_V: Vickers hardness, κ: thermal conductivity obtained by experiment; P_3: total scattering phonon space value, V_3: anharmonic amplitude.

	B	G	H_V	κ^a	κ^b	P_3	V_3
	GPa	GPa	GPa	$Wm^{-1}K^{-1}$	$Wm^{-1}K^{-1}$	10^{-4} cm	10^{19}
Diamond	443[d]	535[d]	96[g]	2270[e]	3450[e]	1.03	2.86
c-BN	400.0[d]	409.0[d]	66[g]	768[e]	2145[e]	1.33	3.50
c-Si_3N_4	303.4[f]	247.5[f]	34.9[f]	23.0[c]	88[c]	2.72	5.51

[a] Measured values by experiments.
[b]Therorectical values for single-crystalline materials.
[c]This work.
[d]Reference [3].
[e]Reference [4] (single crystals).
[f]Reference [2].
[g]Reference [13].

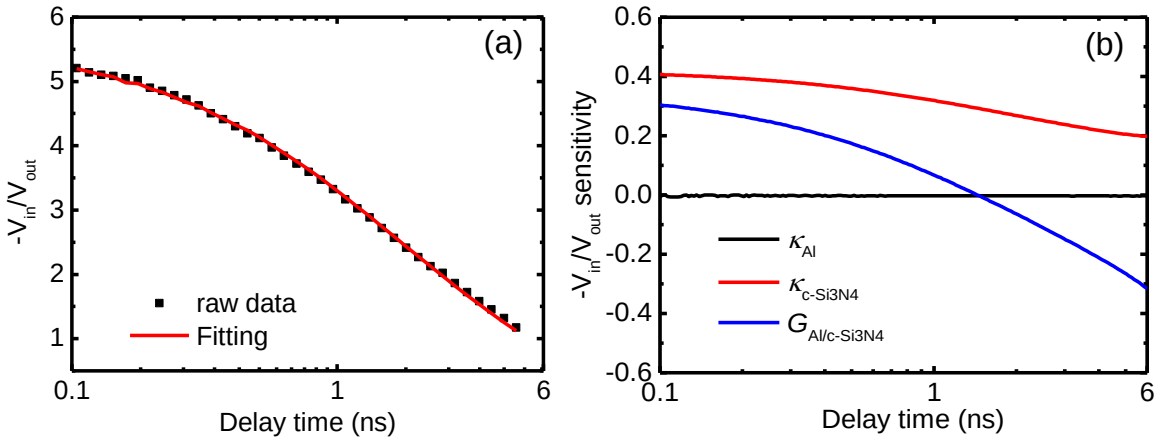

FIG. 1 (a) $-V_{in}/V_{out}$ signal fitting for Al on c-Si_3N_4 with two-unknown parameters: thermal conductivity of c-Si_3N_4, and interface thermal conductance between Al and c-Si_3N_4. Here V_{in} and V_{out} are the in-phase and out-of-phase of the detected signal in the time-domain thermoreflectance (TDTR) measurement, respectively. (b) The sensitivities of $-V_{in}/V_{out}$ signal to the properties. The red line and the blue line represent the sensitivity of thermal conductivity of c-Si_3N_4 and the interface thermal conductance between Al and c-Si_3N_4.

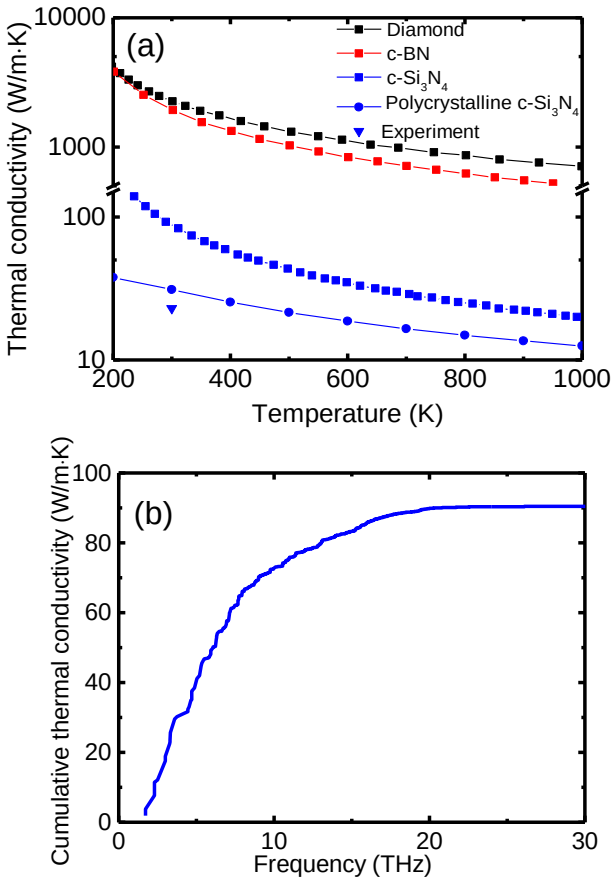

FIG. 2 (a) The squares are the temperature dependences of thermal conductivity of single crystalline c-Si_3N_4, diamond [34, 40] and c-BN [31] obtained by first-principles calculations. The circles are the thermal conductivity of polycrystalline c-Si_3N_4 calculated by adopting an empirical model. The triangle is the thermal conductivity of polycrystalline c-Si_3N_4 obtained by the time-domain thermoreflectance (TDTR) method. (b) Dependence of cumulative thermal conductivity on frequency for c-Si_3N_4.

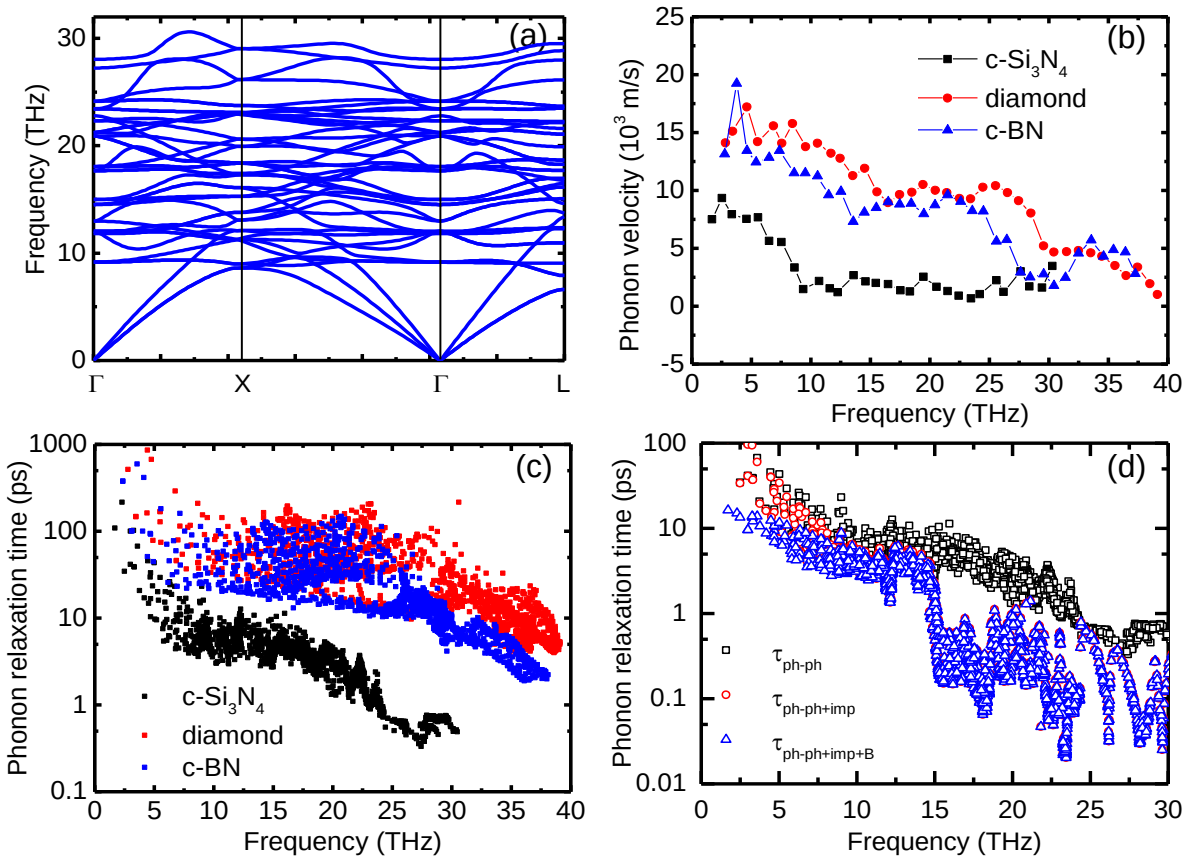

FIG. 3 (a) Dispersion relations of single crystal c-Si_3N_4. (b) Frequency-dependent phonon group velocity and (c) relaxation time for single crystal c-Si_3N_4, diamond, and c-BN. (d) Relaxation times of single crystalline c-Si_3N_4 and polycrystalline c-Si_3N_4, where subscripts ph-ph, imp, and B denote phonon-phonon scattering, phonon-impurity scattering, and phonon-boundary scattering, respectively.

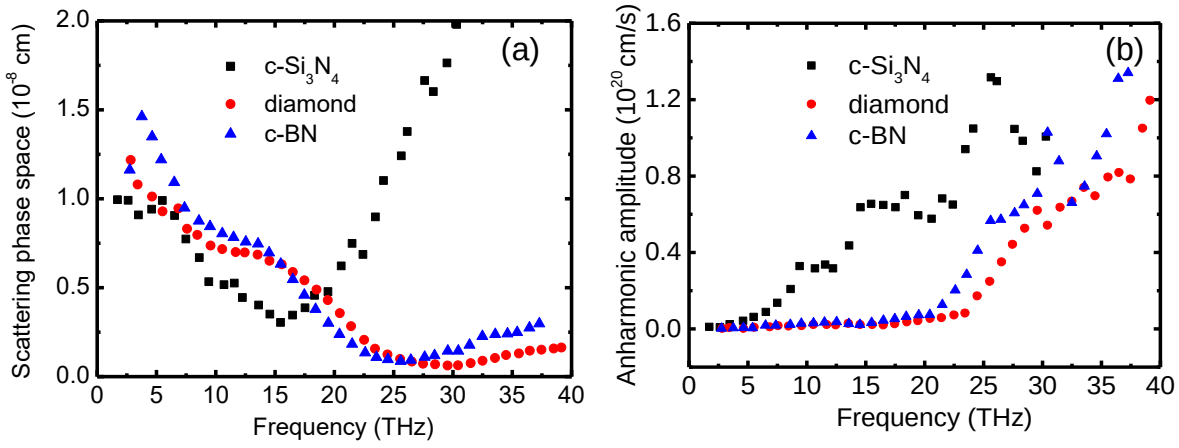

FIG. 4. Comparison of (a): SPS (P_3) and (b): anharmonic amplitude (V_3) in frequency domain for single crystal c-Si_3N_4, diamond, and c-BN.

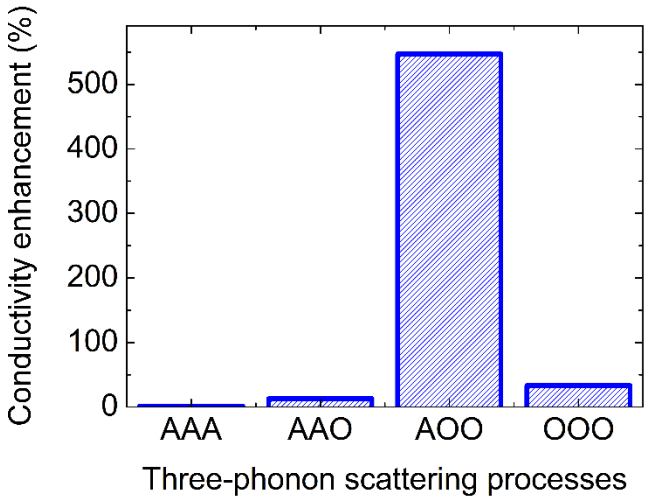

FIG. 5. Analysis of the impact of different groups of three-phonon scattering processes on thermal conductivity by evaluating the enhancement when turning off the processes. “A” and “O” denote acoustic and optical phonon, respectively.

References:

[1] F. Gao, J. He, E. Wu, S. Liu, D. Yu, D. Li, S. Zhang, and Y. Tian, *Hardness of covalent crystals*, Phys Rev Lett **91**, 015502 (2003).

[2] N. Nishiyama, R. Ishikawa, H. Ohfuji, H. Marquardt, A. Kurnosov, T. Taniguchi, B. N. Kim, H. Yoshida, A. Masuno, J. Bednarcik, E. Kulik, Y. Ikuhara, F. Wakai, and T. Irifune, *Transparent polycrystalline cubic silicon nitride*, Sci Rep **7**, 44755 (2017).

[3] D. M. Teter, *Computational alchemy: The search for new superhard materials*, Mrs Bulletin **23**, 22 (1998).

[4] L. Lindsay, D. A. Broido, and T. L. Reinecke, *First-principles determination of ultrahigh thermal conductivity of boron arsenide: a competitor for diamond?*, Phys Rev Lett **111**, 025901 (2013).

[5] D. G. Onn, A. Witek, Y. Z. Qiu, T. R. Anthony, and W. F. Banholzer, *Some Aspects of the Thermal-Conductivity of Isotopically Enriched Diamond Single-Crystals*, Physical Review Letters **68**, 2806 (1992).

[6] L. H. Wei, P. K. Kuo, R. L. Thomas, T. R. Anthony, and W. F. Banholzer, *Thermal-Conductivity of Isotopically Modified Single-Crystal Diamond*, Physical Review Letters **70**, 3764 (1993).

[7] D. A. S. S. Mukhopadhyay, *Polar Effects on the Thermal Conductivity of Cubic Boron Nitride under Pressure*, Physical Review Letters **113**, 025901 (2014).

[8] S. G. A., *Nonmetallic Crystals with High Thermal-Conductivity*, Journal of Physics and Chemistry of Solids **34**, 321 (1973).

[9] T. L. Feng, L. Lindsay, and X. L. Ruan, *Four-phonon scattering significantly reduces intrinsic thermal conductivity of solids*, Physical Review B **96** 161201(R) (2017).

[10] F. Tian, B. Song, X. Chen, N. K. Ravichandran, Y. C. Lv, K. Chen, S. Sullivan, J. Kim, Y. Y. Zhou, T. H. Liu, M. Goni, Z. W. Ding, J. Y. Sun, G. A. G. U. Gamage, H. R. Sun, H. Ziyaee, S. Y. Huyan, L. Z. Deng, J. S. Zhou, A. J. Schmidt, S. Chen, C. W. Chu, P. S. E. Y. Huang, D. Broido, L. Shi, G. Chen, and Z. F. Ren, *Unusual high thermal conductivity in boron arsenide bulk crystals*, Science **361**, 582 (2018).

[11] Q. Z. Sheng Li, Yinchuan Lv, Xiaoyuan Li, Xiqu Wang, Pinshane Y. Huang, David G. Cahill, Bing Lv, *High thermal conductivity in cubic boron arsenide crystals*, Science **361**, 579 (2018).

[12] J. S. Kang, M. Li, H. Wu, H. Nguyen, and Y. Hu, *Experimental observation of high thermal conductivity in boron arsenide*, Science **361**, 575 (2018).

[13] W. G. Zeier, A. Zevalkink, Z. M. Gibbs, G. Hautier, M. G. Kanatzidis, and G. J. Snyder, *Thinking Like a Chemist: Intuition in Thermoelectric Materials*, Angewandte Chemie-International Edition **55**, 6826 (2016).

[14] T. T. Jia, G. Chen, and Y. S. Zhang, *Lattice thermal conductivity evaluated using elastic properties*, Physical Review B **95** 155206 (2017).

[15] A. Zerr, G. Miehe, G. Serghiou, M. Schwarz, E. Kroke, R. Riedel, H. Fuess, P. Kroll, and R. Boehler, *Synthesis of cubic silicon nitride*, Nature **400**, 340 (1999).

[16] D. R. Lide, *CRC Handbook of Chemistry and Physics* (CRC Press, Boca Raton, 2005), Internet Version edn., Vol. 9, p.^pp. 53.

[17] D. R. Lide, *CRC Handbook of Chemistry and Physics* (CRC Press, Boca Raton, 2005), Internet Version edn., Vol. 9, p.^pp. 56.

[18] A. T. Kazuyoshi Tatsumi, Isao Tanaka, *First-principles calculation of the lattice thermal conductivities of α-, β-, and γ-Si3N4*, arXiv: 1612.08480, 2016.
[19] M. Schwarz, G. Miehe, A. Zerr, E. Kroke, B. T. Poe, H. Fuess, and R. Riedel, *Spinel-Si3N4: Multi-anvil press synthesis and structural refinement*, Advanced Materials **12**, 883 (2000).
[20] D. G. Cahill, W. K. Ford, K. E. Goodson, G. D. Mahan, A. Majumdar, H. J. Maris, R. Merlin, and P. Sr, *Nanoscale thermal transport*, Journal of Applied Physics **93**, 793 (2003).
[21] D. G. Cahill, K. E. Goodson, and A. Majumdar, *Thermometry and thermal transport in micro/nanoscale solid-state devices and structures*, Journal of Heat Transfer-Transactions of the Asme **124**, 223 (2002).
[22] T. Oyake, M. Sakata, and J. Shiomi, *Nanoscale thermal conductivity spectroscopy by using gold nano-islands heat absorbers*, Applied Physics Letters **106**, 073102 (2015).
[23] K. Esfarjani and H. T. Stokes, *Method to extract anharmonic force constants from first principles calculations*, Physical Review B **77**, 144112 (2008).
[24] K. Esfarjani, G. Chen, and H. T. Stokes, *Heat transport in silicon from first-principles calculations*, Physical Review B **84** (2011).
[25] J. Shiomi, K. Esfarjani, and G. Chen, *Thermal conductivity of half-Heusler compounds from first-principles calculations*, Physical Review B **84**, 085204 (2011).
[26] P. Giannozzi, S. Baroni, N. Bonini, M. Calandra, R. Car, C. Cavazzoni, D. Ceresoli, G. L. Chiarotti, M. Cococcioni, I. Dabo, A. Dal Corso, S. de Gironcoli, S. Fabris, G. Fratesi, R. Gebauer, U. Gerstmann, C. Gougoussis, A. Kokalj, M. Lazzeri, L. Martin-Samos, N. Marzari, F. Mauri, R. Mazzarello, S. Paolini, A. Pasquarello, L. Paulatto, C. Sbraccia, S. Scandolo, G. Sclauzero, A. P. Seitsonen, A. Smogunov, P. Umari, and R. M. Wentzcovitch, *QUANTUM ESPRESSO: a modular and open-source software project for quantum simulations of materials*, J Phys Condens Matter **21**, 395502 (2009).
[27] J. P. Perdew, A. Ruzsinszky, G. I. Csonka, O. A. Vydrov, G. E. Scuseria, L. A. Constantin, X. L. Zhou, and K. Burke, *Restoring the density-gradient expansion for exchange in solids and surfaces*, Physical Review Letters **100**, 136406 (2008).
[28] T. Tadano, Y. Gohda, and S. Tsuneyuki, *Anharmonic force constants extracted from first-principles molecular dynamics: applications to heat transfer simulations*, J Phys Condens Matter **26**, 225402 (2014).
[29] S. Tamura, *Isotope Scattering of Dispersive Phonons in Ge*, Physical Review B **27**, 858 (1983).
[30] Z. F. Huimin Xiang, Zhongping Li& Yanchun Zhou, *Theoretical predicted high-thermalconductivity cubic Si3N4 and Ge3N4: promising substrate materials for high-power electronic devices*, Scientific Reports **8**, 14374 (2018).
[31] D. T. Morelli, J. P. Heremans, and G. A. Slack, *Estimation of the isotope effect on the lattice thermal conductivity of group IV and group III-V semiconductors*, Physical Review B **66**, 195304 (2002).
[32] T. Feng and X. Ruan, *Quantum mechanical prediction of four-phonon scattering rates and reduced thermal conductivity of solids*, Physical Review B **93**, 045202 (2016).
[33] Q. Y. Zheng, C. H. Li, A. Rai, J. H. Leach, D. A. Broido, and D. G. Cahill, *Thermal conductivity of GaN, (GaN)-Ga-71, and SiC from 150 K to 850 K*, Physical Review Materials **3**, 014601 (2019).

[34] G. X. Pranay Chakraborty, Lei Cao, and Yan Wang, *Lattice thermal transport in superhard hexagonal diamond andwurtzite boron nitride: A comparative study with cubic diamond andcubic boron nitride*, Carbon **139**, 85 (2018).
[35] A. Ward and D. A. Broido, *Intrinsic phonon relaxation times from first-principles studies of the thermal conductivities of Si and Ge*, Physical Review B **81**, 085205 (2010).
[36] S. Ju, T. Shiga, L. Feng, and J. Shiomi, *Revisiting PbTe to identify how thermal conductivity is really limited*, Physical Review B **97**, 184305 (2018).
[37] L. Lindsay and D. A. Broido, *Three-phonon phase space and lattice thermal conductivity in semiconductors*, Journal of Physics-Condensed Matter **20**, 165209 (2008).
[38] See Supplemental Material at [URL will be inserted by publisher] for calculation of average anharmonic amplitude in frequency domain.
[39] T. Shiga, T. Murakami, T. Hori, O. Delaire, and J. Shiomi, *Origin of anomalous anharmonic lattice dynamics of lead telluride*, Applied Physics Express **7**, 041801 (2014).
[40] A. Ward, D. A. Broido, D. A. Stewart, and G. Deinzer, *Ab initio theory of the lattice thermal conductivity in diamond*, Physical Review B **80**, 125203 (2009).